support

ISON-NM Observatory capabilities for Gaia-FUN-SSO

CoLiTeC image processing pipeline for moving objects detection

L. Elenin[1], V. Savanevych[2], I. Molotov[1], A. Kozhukhov[3], A. Bryukhovetskiy[3], V. Vlasenko[3], E. Dikov[4], A. Yudin[1]

[1]Keldysh Institute of Applied Mathematics RAS (Russia)

[2]Kharkiv National University of Radioelectronics (Ukraine)

[3]National Centre of Space Devices Control and Test (Ukraine)

[4]Research and Design Institute o (Ukraine)

Location

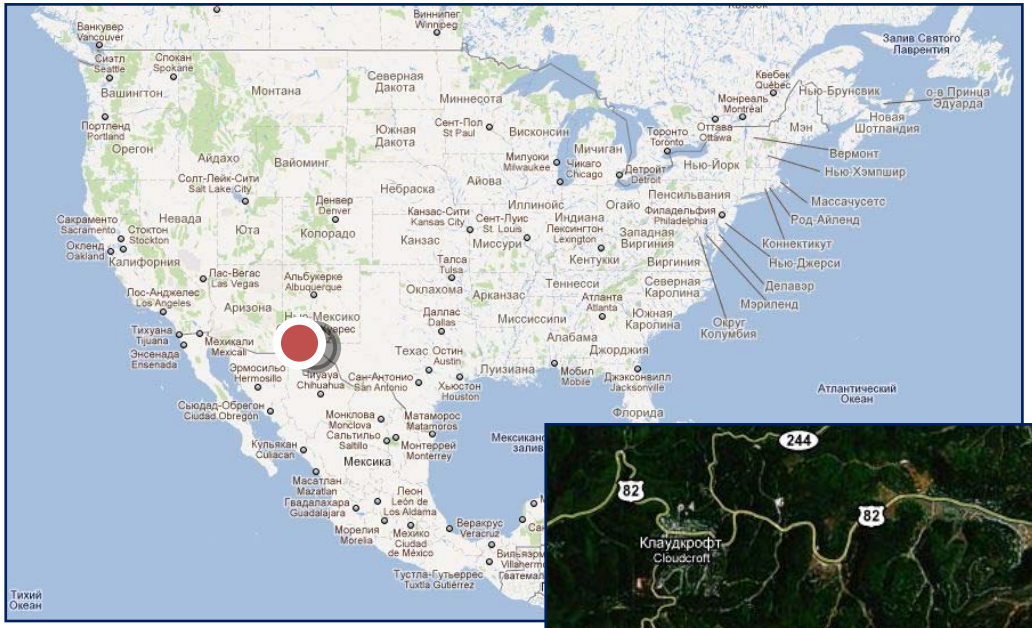

ISON-NM Observatory (H15)

Coordinates:

32° 54′ 11.79″ N

105° 31′ 42.40″ W

2217m above sea level

Distance to observer – 9500 km

Location

Why NMSkies?

Astroclimate

- Many clear nights (260-270 per year)
- Really dark skies (average SQM ~ 22.1 mag/arcsec²)

First light only in 5 month

- Ready infrastructure (fast Internet)
- Experienced support for remote observations

Telescope

Centurion-18

Aperture – 455 mm
Focus lenght – 1270 mm
Focal ratio – f/2.8
CCD – FLI ML09000-65
FOV – 100'x100'
Image scale – 1.95"/pix
Without filter wheel

Main tasks

1. Survey for a new Solar System objects, include near-Earth objects

2. **Follow-up observations of NEA and comets**

3. NEAs photometry

4. Optical transients observation, include working with VOEvent
    1. Gamma-ray bursts
    2. Supernovae
    3. Novae
    4. Cataclysmic variables stars and other transients

5. Supernovae survey*

6. Patrol of cataclysmic variables stars*

7. Photometry of variable stars on survey's images*

** - as by-product, this plans for the near future*

Observatory control

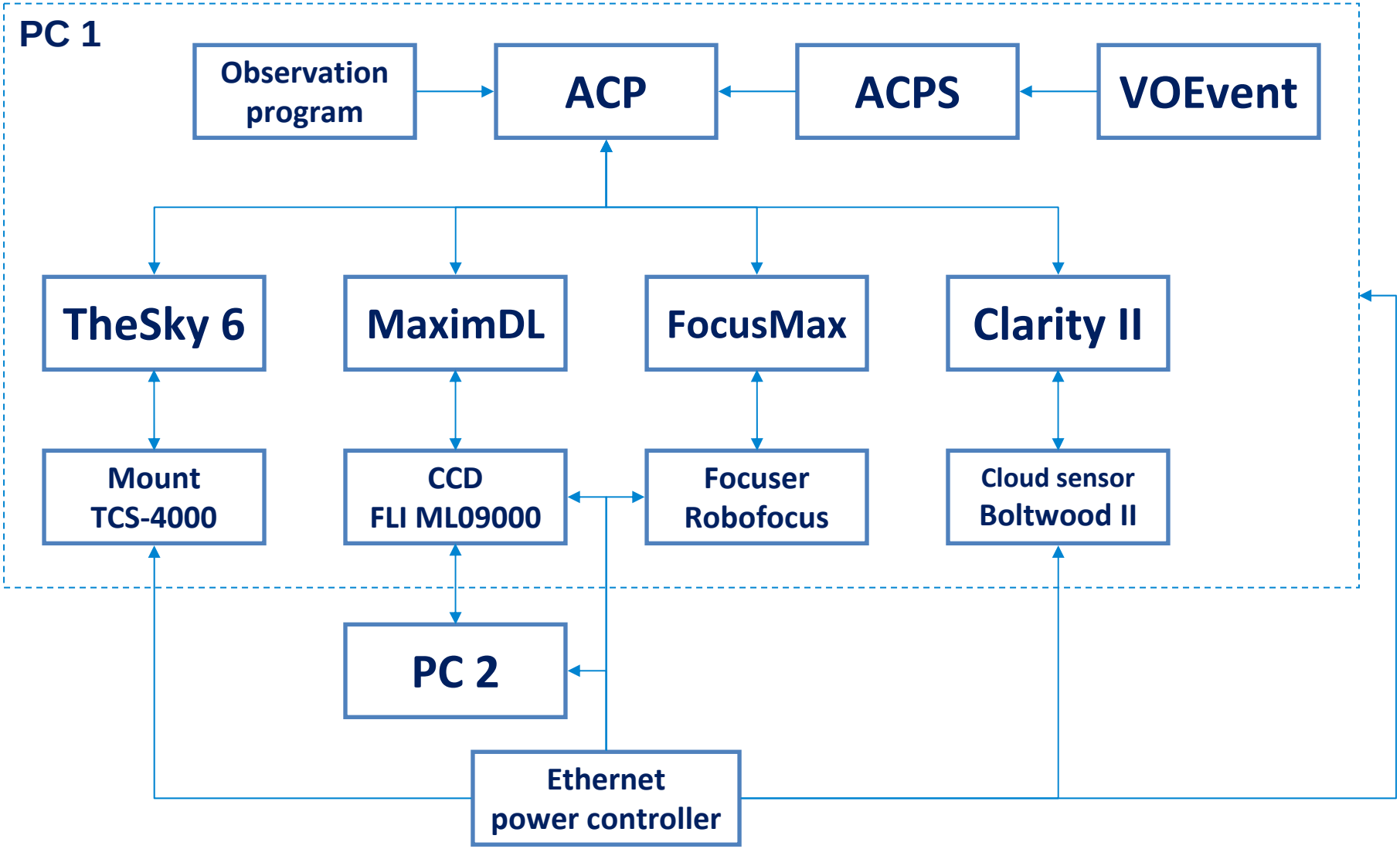

Image processing pipeline - CoLiTeC

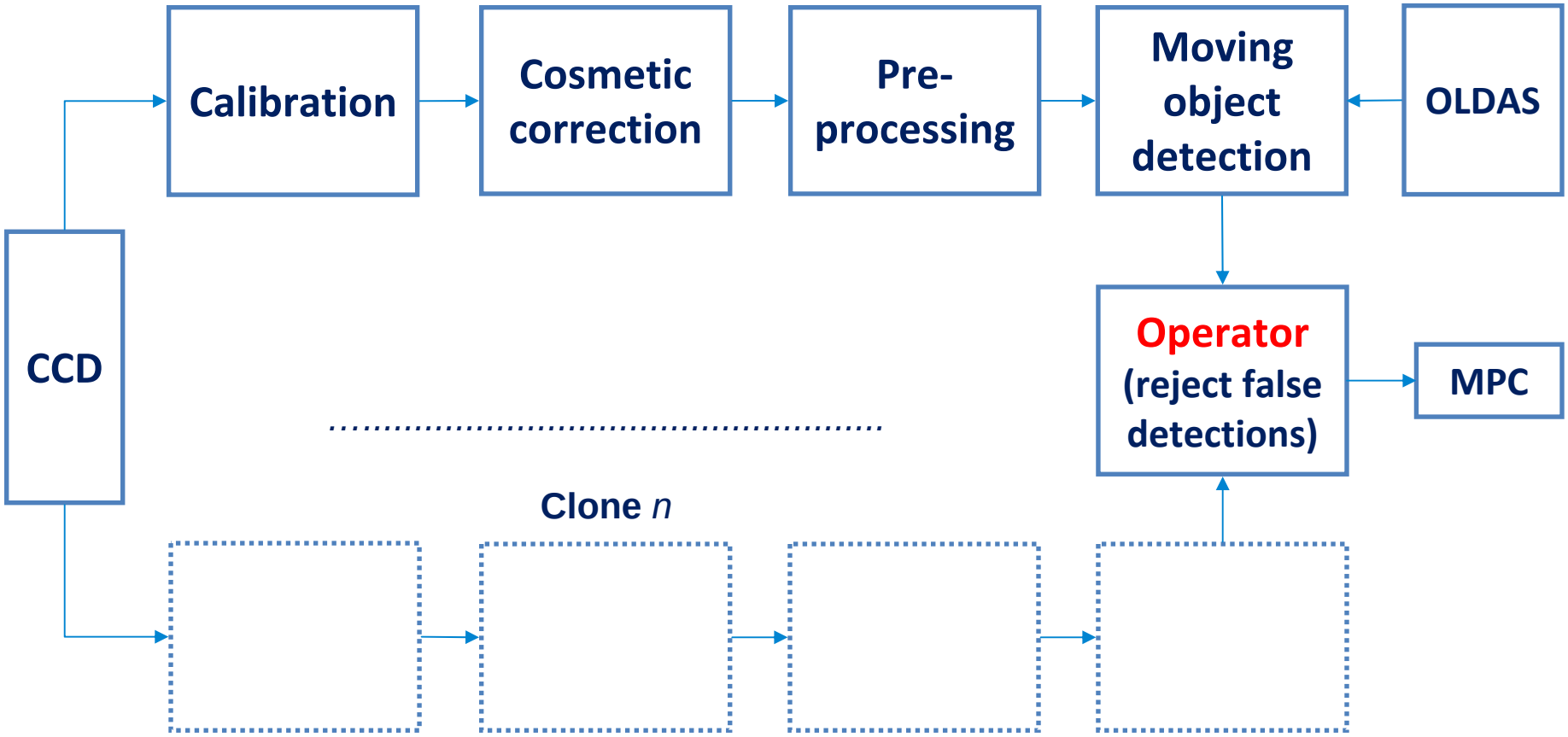

CoLiTec features

1. Automatic detection faint moving objects (SNR>2.5)
2. Working with very wide field of view (up to 10 degrees^2)
3. Auto calibration and cosmetic correction
4. Fully automatic robust algorithm of astrometric reduction
5. Automatic rejection of objects with worst observations
6. Results viewer (CLT-Viewer) with graphical user interface
7. Multi-threaded support for multi-cores systems and local network
8. Processing pipeline managed by OLDAS (OnLine Data Analysis System)

** - plans for the near future*

More detailed presentation about CoLiTec software available on demand

Scheme of CCD-frame's formation with display of asteroid

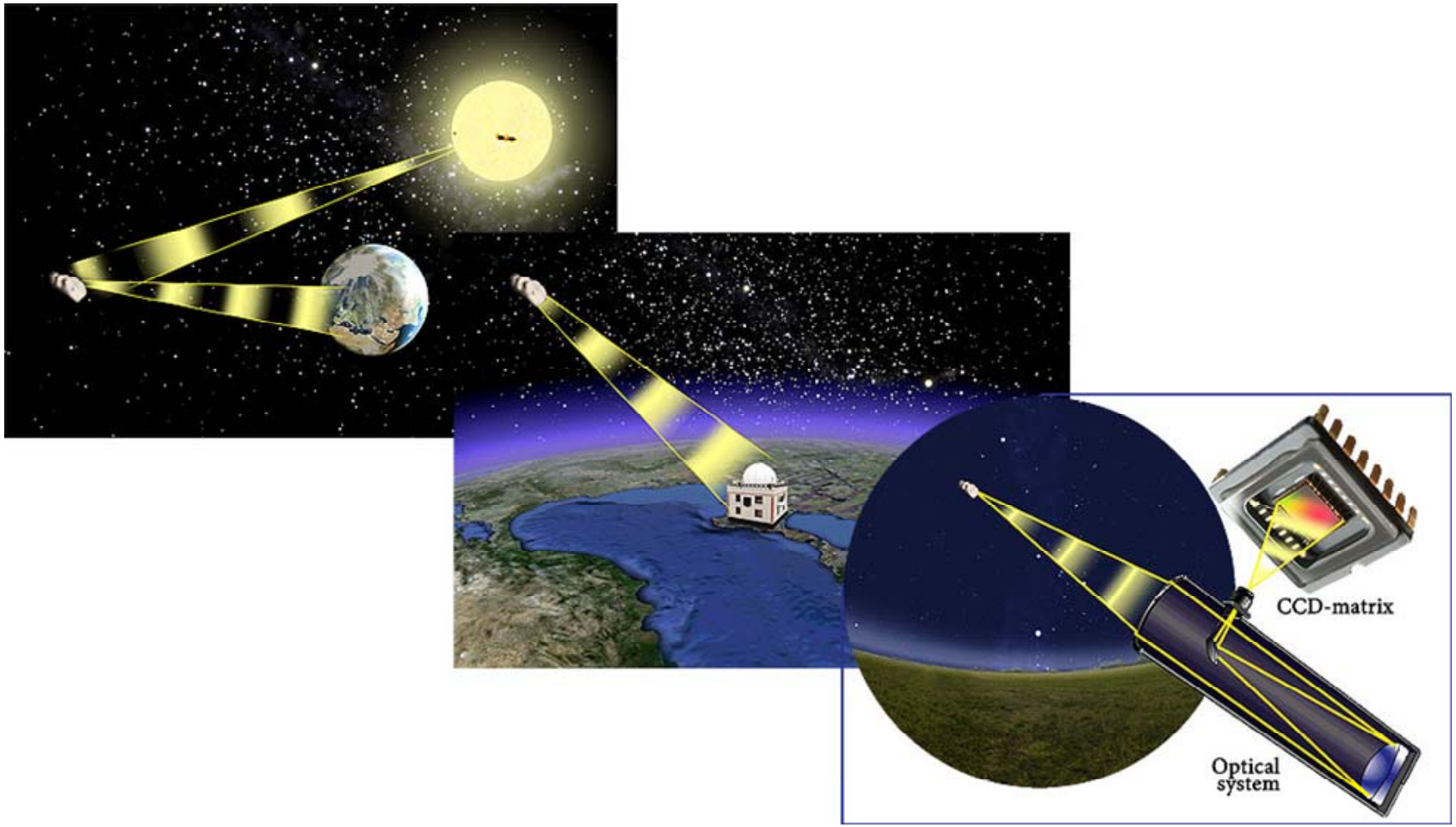

Method of CCD-frames' stacking with signal's accumulation from a faint asteroid with nonzero apparent motion on series of CCD-frames (method FSMO)

The present method differs from others in following:

- mutual matching of marks identified with star catalog on the basic and stacking frames is used to estimate frames' mutual shift;
- record of stacking frames' mutual shift fractioning and asteroid's moving direction is carrying out using "areal" approach (weighting matrix);
- blurring matrix is used to increase efficiency of asteroid signal's amplitude accumulation in presence of residual errors of adding frames' mutual shift estimation.
- estimation of the best value of blurring matrix' elements is done using method of simulation on experimental data.

This method is used in FSMO frames' block of subseries model's intraframe CoLiTec processing. It permits to increase relation "signal/noise" of signals from faint asteroids and unknown parameters of motion on CCD-frame.

Introduction of the **method for combination of superframes** from same subseries.

The present method is based on assumption that signal of only one asteroid can get into the same area of a small size frame. Application of this method permits to increase quality level of asteroids' tracks detection and to cut down computational cost of asteroids' detection on obtained superframes.

CCD-frames' stacking with signal's accumulation from a faint asteroid with nonzero apparent motion

Estimation of current frame's central coordinate's shift from basic frame's central coordinates

$$\begin{cases} dx_{et} = \dfrac{1}{N'_{bl}} \sum\limits_{i=1}^{i=N'_{bl}} \sum\limits_{j=1}^{j=N'_{bl}} (x_{jt} - x_{ib}); \\ dy_{et} = \dfrac{1}{N'_{bl}} \sum\limits_{i=1}^{i=N'_{bl}} \sum\limits_{j=1}^{j=N'_{bl}} (y_{jt} - y_{ib}), \end{cases} \tag{1.1}$$

where dx_{et}, dy_{et} – used estimation of current frame's central coordinate's shift from basic frame's central coordinates; x_{ib}, y_{ib} – coordinates of basic frame's i-й mark; x_{jt}, y_{jt} – coordinates of current frame's j-й mark matching basic frame's i - mark; N'_{bl} – quantity of mutually matching couples of marks.

FSMO in fractional shift between frames.

$$A_{\Sigma ik} = \sum_{t=t_1}^{t_1+N_{stack}-1} \sum_{e=0}^{1} \sum_{g=0}^{1} \gamma_{egt} \cdot A_{(i+\Delta N_{xt}+e\cdot j_{xt}),(k+\Delta N_{yt}+g\cdot j_{yt})t} \tag{1.2}$$

$$\text{where } \gamma_t = \begin{pmatrix} \gamma_{00t} & \gamma_{01t} \\ \gamma_{10t} & \gamma_{11t} \end{pmatrix}; \tag{1.3}$$

$$\gamma_{00t} = (1-|d\Delta x_t|)(1-|d\Delta y_t|); \quad \gamma_{10t} = |d\Delta x_t|(1-|d\Delta y_t|); \quad \gamma_{01t} = (1-|d\Delta x_t|)|d\Delta y_t|; \quad \gamma_{11t} = |d\Delta x_t| \cdot |d\Delta y_t|; \quad d\Delta x_t = \Delta x_t - E(\Delta x_t);$$

$$d\Delta y_t = \Delta y_t - E(\Delta y_t); \; j_{xt} = \begin{cases} -1, & \Delta x_t < 0 \\ 1, & \Delta x_t \geq 0 \end{cases}; \; j_{yt} = \begin{cases} -1, & \Delta y_t < 0 \\ 1, & \Delta y_t \geq 0 \end{cases}$$

“Areal” approach in FSMO

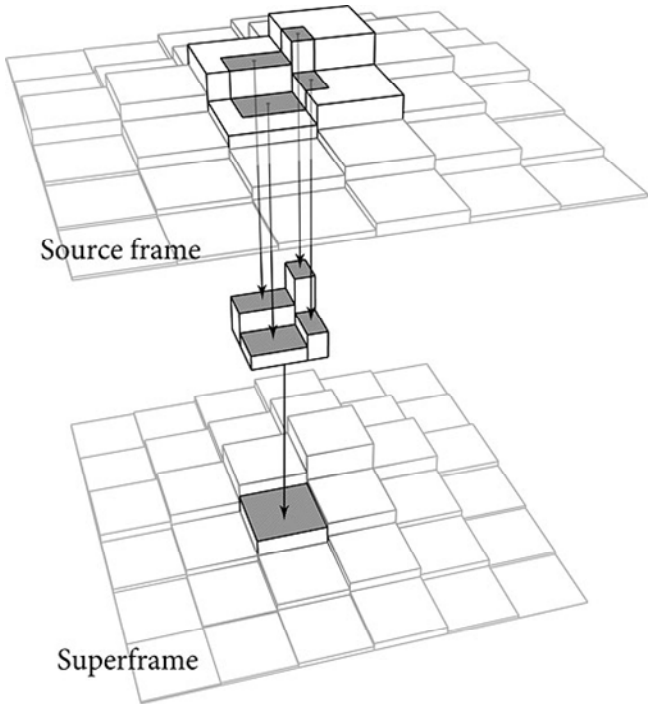

Fig. 1.1 Addition of frames with mutual shift for fractional number of pixels based on “areal” approach

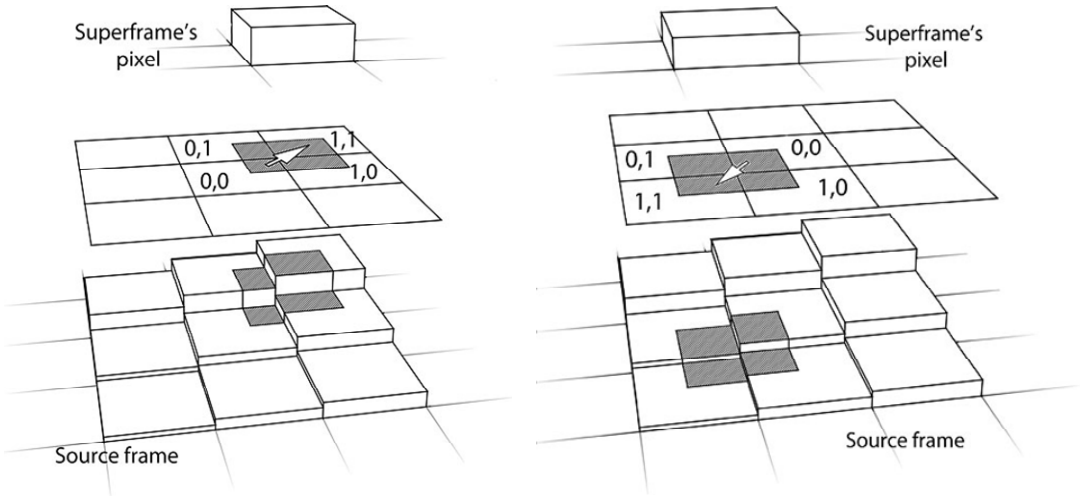

Fig. 1.2 Selection of basic frame’s pixels for FSMO with different shift’s directions of initial frame relative to the basic one

Application of blurring matrix in FSMO in fractional shift between frames

$$A_{\Sigma ik} = \sum_{t=t_1}^{t_1+N_{stack}-1} \sum_{e=0}^{1} \sum_{g=0}^{1} \sum_{j_p=0}^{2n} \sum_{i_p=-n}^{n} \gamma_{egt} \cdot M_{ffj_p(i_p+n)} \cdot A_{(i+i_p+\Delta N_{xt}+e\cdot j_{xt}),(k-j_p+1+\Delta N_{yt}+g\cdot j_{yt})t}\,, \tag{1.4}$$

where $M_f = \begin{pmatrix} \lambda & \beta & \lambda \\ \beta & 1 & \beta \\ \lambda & \beta & \lambda \end{pmatrix}$, $\lambda \le \beta,\ \lambda < 1, \beta \le 1$ (1.5)

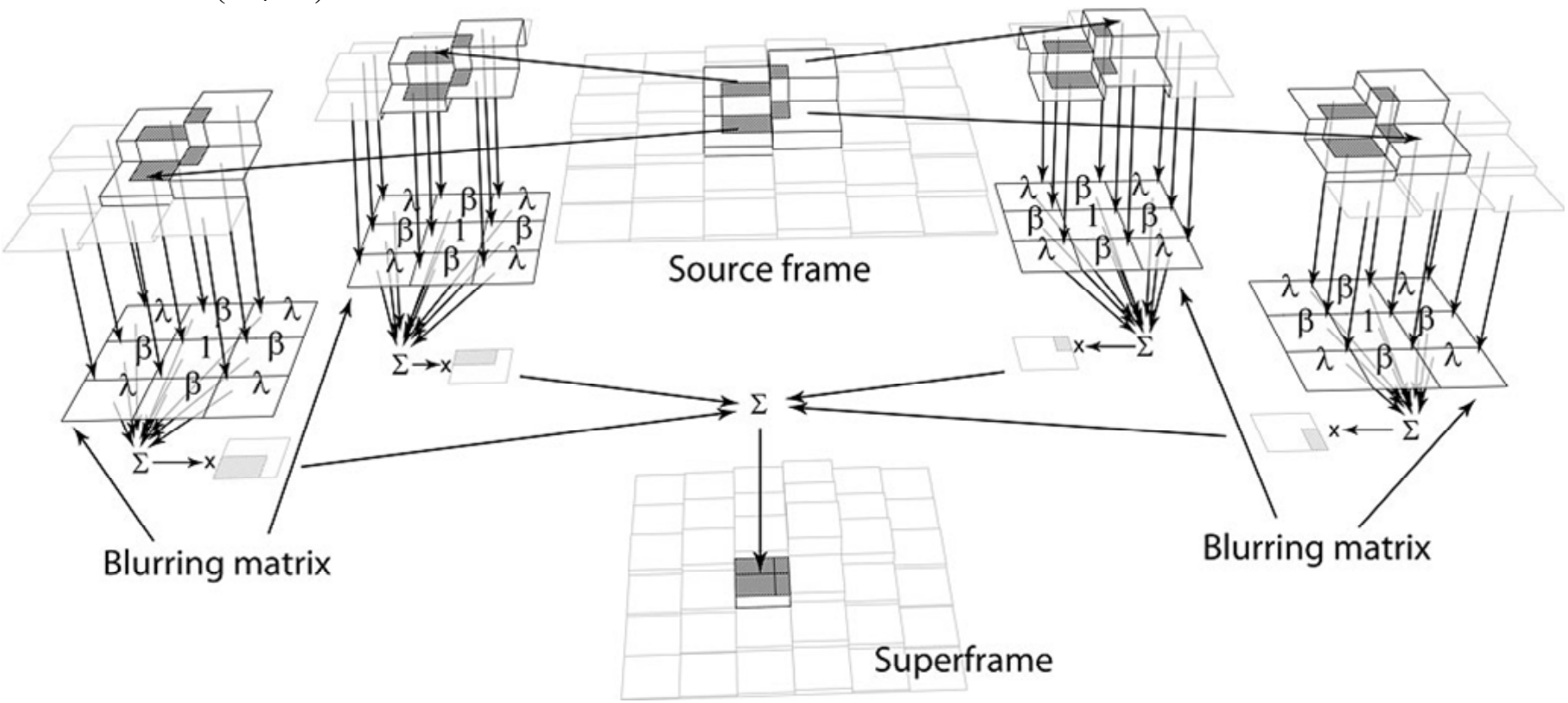

Fig. 1.3 Application of blurring matrix in FSMO

Method for preliminary selection of celestial objects' signals

Method for preliminary selection of celestial objects' signals**.** Method based upon comparison with spatial convolution criteria of received flux (in the vicinity of image peak) with form of estimated signal. Let's suppose that signals from celestial objects are formed around image peaks and value of spatial convolution for "background" image peaks on the frame are distributed according to the normal distribution law. We also assume that spatial form of the signal doesn't depend on its position in pixel during preliminary selection stage and that the estimation of signal's spatial convolution (for each vicinity of image peak) is done once to obtain expected position of the object matching the center of corresponding image peak.

The new distribution model of spatial convolution's values for current frame is used. This model represents mixture of normal distribution law ("background" spatial convolution's values) and "tail" ("signal" spatial convolution's values) in area of spatial convolution's large values.

Approximate selection of normal ("background") component of distribution of spatial convolution's values mixture is used to estimate the rejection threshold for image peaks with no signals from celestial objects in its vicinity. It's done according to the iterative computing circuit, based on property of equality for median's values and mean value for normally distributed random values.

The present method is used in block of preliminary selection of CoLiTec intraframe processing module and it permits to cut down computational cost of estimation of celestial objects' signals location. This method doesn't skip celestial objects' signals which can be stably detected without its application.

Preliminary selection of celestial objects' signals on CCD-frame

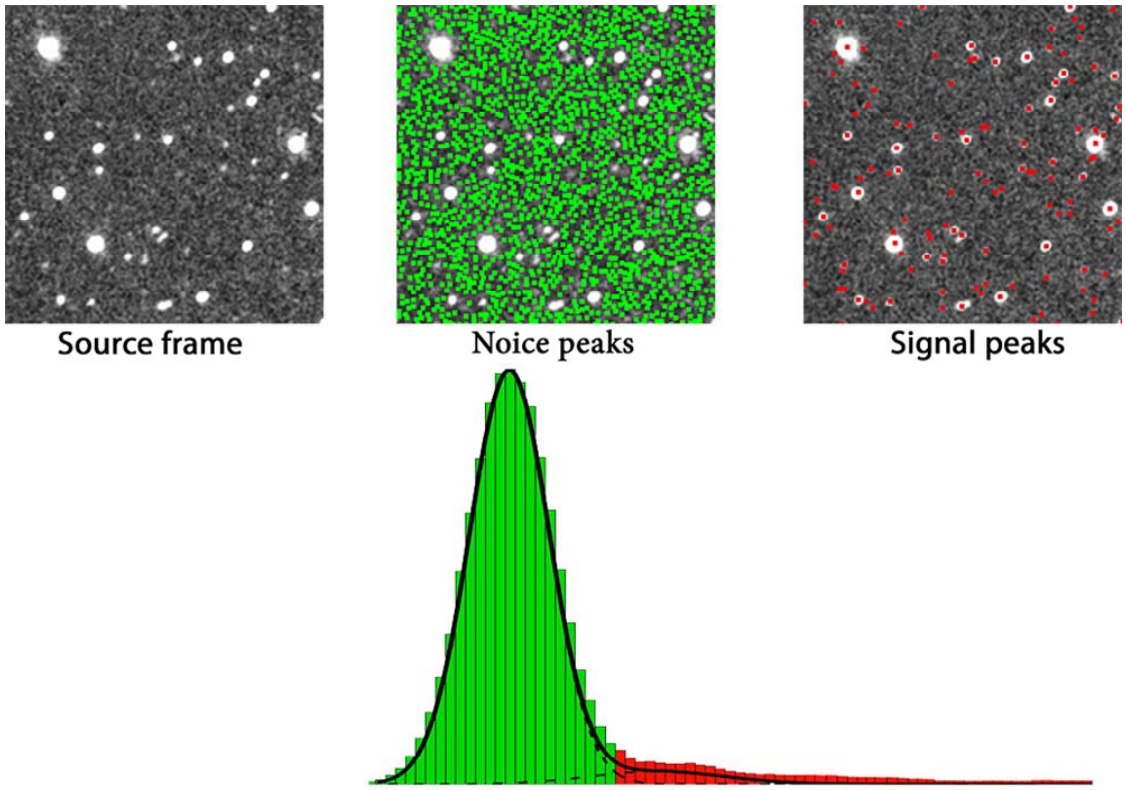

Fig. 2.1 Decision rule for detection of celestial objects' signals

$$A_{it} = \sum_{i,k}^{N_{IPSs}} \upsilon_{ikt} A_{ikt} > Tr_1 \qquad (2.1)$$

where – A_{it} amplitude of signals for detection; N_{IPSs} – number of pixels in intraframe processing strobe with expected signal; A_{ikt} – amplitude of ik-pixel of t CCD-frame.

Estimation of the rejection threshold's value for image peaks

Mean value of spatial convolution of received radiation and mask matching the form of expected signal.

$$\overline{A}_{\ell t} = \left(\sum_{j=1}^{j=N_{\max \ell t}^{\ell oc}} A_{jt} \right) / N_{\max \ell t}^{\ell oc}, \tag{2.2}$$

where $N_{\max \ell t}^{\ell oc}$ – quantity of local maximums at ℓ-iteration of the method on the t frame; $\overline{A}_t$ – mean value of spatial convolution at ℓ - iteration of the method on the t frame; A_{jt} – value of spatial convolution for j-peak on the t-frame.

Mean square deviation of convolution's values of received radiation and mask matching the form of expected signal

$$\sigma_{eA\ell t} = \sqrt{\sum_{j=1}^{j=N_{\max \ell t}^{\ell oc}} (A_{jt} - \overline{A}_{\ell t})^2 / (N_{\max \ell t}^{\ell oc} - 1)} \tag{2.3}$$

Condition of value's elimination of spatial convolution of received radiation and mask matching the form of expected signal

$$A_{jt} \geq \overline{A}_{\ell t} + 3\sigma_{eA\ell t} \tag{2.4}$$

Rejection threshold's value

$$L_1 = \overline{A}_{\ell t} + k_{rej}\sigma_{eA\ell t}, \tag{2.5}$$

where k_{rej} - proportionality constant (usually in the range of 2 and 3) experimentally identified for each telescope with CCD-camera.

Iterative method of estimation of asteroid's coordinates on the discrete image.

Iterative method of estimation of asteroid's coordinates on the discrete image. Method represents estimation of asteroid's coordinates on the discrete image, considering estimation of continuous parameters (asteroids' coordinates) on the discrete image (set of CCD-matrix pixels' potentials) and the fact that residual noise photons can be unevenly distributed on an object's image. For the first time in grouped samples' technology, the present method expands the model of noise photons' coordinates decreasing to the noise flat substrate with parameters permanent in the range of examined strobe.

The present method is used in coordinates' estimation block and module's signal amplitude of CoLiTec intraframe processing. It permits to obtain estimations of signals' coordinates from celestial objects on CCD-frame to tenth pixel's part.

The estimation of celestial objects' equatorial coordinates on CCD-frame is done according to the estimation of coordinates obtained. For this purpose, the standard coordinates of the asteroid have to be defined through generalized least squares (GLS) estimation of plates' constants. After that, the ideal coordinates have to be converted into equatorial. Formation of weighting generic GLS matrix of measurement's errors was completed accounting dependence of errors in equatorial coordinates' estimation upon apparent brightness of reference stars. Also, the novelty of the method is arrangement of reference stars' even choice and application of several iterations of LSM-estimation rejecting abnormal data. Such approach favours the increase of precision and reliability of estimation of plate's constants, especially when models of plate's constants with a degree higher than the first one are used.

The method is used in estimation block of marks' equatorial coordinates from CoLiTec intraframe processing module. It permits to obtain estimation of asteroids' equatorial coordinates with a precision accepted by Minor Planet Center (MPC).

Estimation of asteroid's coordinates on the discrete image

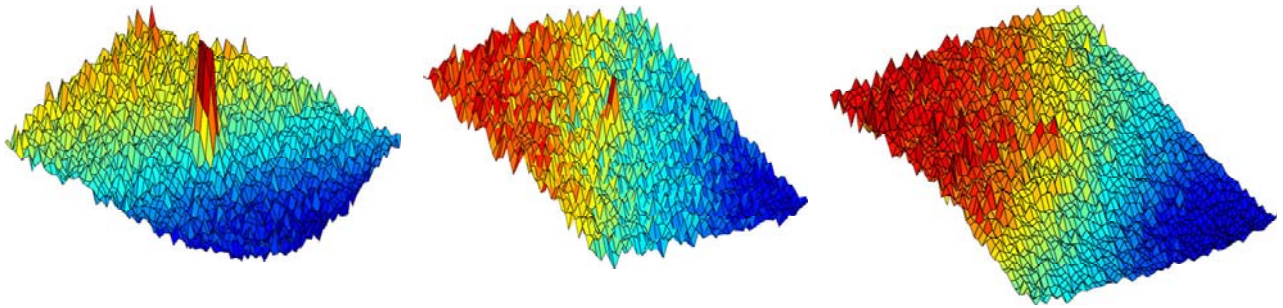

Fig. 3.1 Types of asteroids' signals

The law of distribution of photons' fall on CCD-matrix

$$f(x,y) = A_{noise}\,x + B_{noise}\,y + C_{noise} + \frac{p_1}{2\pi\sigma_{ph}^2}\exp\left\{-\frac{1}{2\sigma_{ph}^2}\left[(x-x_t)^2 + (y-y_t)^2\right]\right\} \quad (3.1)$$

where $p_1 = 1 - p_0$ – relative weight of signal photons; $p_0 = \int_{x_{begi}}^{x_{endi}}\int_{y_{begk}}^{y_{endk}}(A_{noise}\,x + B_{noise}\,y + C_{noise})\,dxdy$ – relative weight of CCD-matrix noise photons; $A_{noise}, B_{noise}, C_{noise}$ – parameters of noise flat substrate; σ_{ph} – Stdev of signal photons' fall coordinates; x_t, y_t – coordinates of celestial object on t-frame.

Relative frequency of photons' fall in ik-pixel of CCD-matrix in t-frame:

$$\upsilon^*_{ikt} = \frac{A_{ikt}}{\sum_{i,k}^{N_{IPS}} A_{ikt}} \quad (3.2)$$

Probability of photons getting into ik-pixel of CCD-matrix in t-frame:

$$\upsilon_{ikt}(\Theta) = \int_{x_{begi}}^{x_{endi}}\int_{y_{begk}}^{y_{endk}} f(x,y)\,dxdy \quad (3.3)$$

Probability function:

$$L_t(\Theta) = \prod_{i,k}^{N_{CCD}} \upsilon_{ikt}^{\vartheta_{ikt}}(\Theta) \xrightarrow[x_t, y_t]{} \max \quad (3.4)$$

Estimation of asteroid's coordinates on the discrete image (continuation)

Estimation of signal's coordinates from an asteroid in CCD-frame's coordinate system.

$$\begin{cases} x_{et} = \dfrac{\sum\limits_{i,k}^{N_{IPSs}} \upsilon^{*}_{ikts}\lambda_{ikt} m^{\ell oc}_{x_i}}{\sum\limits_{i,k}^{N_{IPSs}} \upsilon^{*}_{ikts}\lambda_{ikt}}; \\ y_{et} = \dfrac{\sum\limits_{i,k}^{N_{IPSs}} \upsilon^{*}_{ikts}\lambda_{ikt} m^{\ell oc}_{y_k}}{\sum\limits_{i,k}^{N_{IPSs}} \upsilon^{*}_{ikts}\lambda_{ikt}}; \end{cases} \qquad (3.5)$$

Estimation of mean square deviation asteroid's signal in CCD-frame's coordinate system

$$\sigma^2_{eph} \approx \frac{\sum\limits_{i,k}^{N_{IPSs}} \upsilon^{*}_{ikts}\lambda_{ikt}\left(\left(m^{\ell oc}_{xi} - x_{et}\right)^2 + \left(m^{\ell oc}_{yk} - y_{et}\right)^2\right)}{2\sum\limits_{i,k}^{N_{IPSs}} \upsilon^{*}_{ikts}\lambda_{ikt}}, \qquad (3.6)$$

where $\lambda_{ikt} = \dfrac{p_{e1} F_{yk}(y_t;\sigma^2_{ph}) F_{xi}(x_t;\sigma^2_{ph})}{\upsilon_{ikts}(\Theta)}$ (3.7); $\qquad p_{e1} = \dfrac{1}{N_{IPSs}} \sum\limits_{i,k}^{N_{IPSs}} \lambda_{ikt}$ (3.8).

Estimation of noise flat substrate's parameters

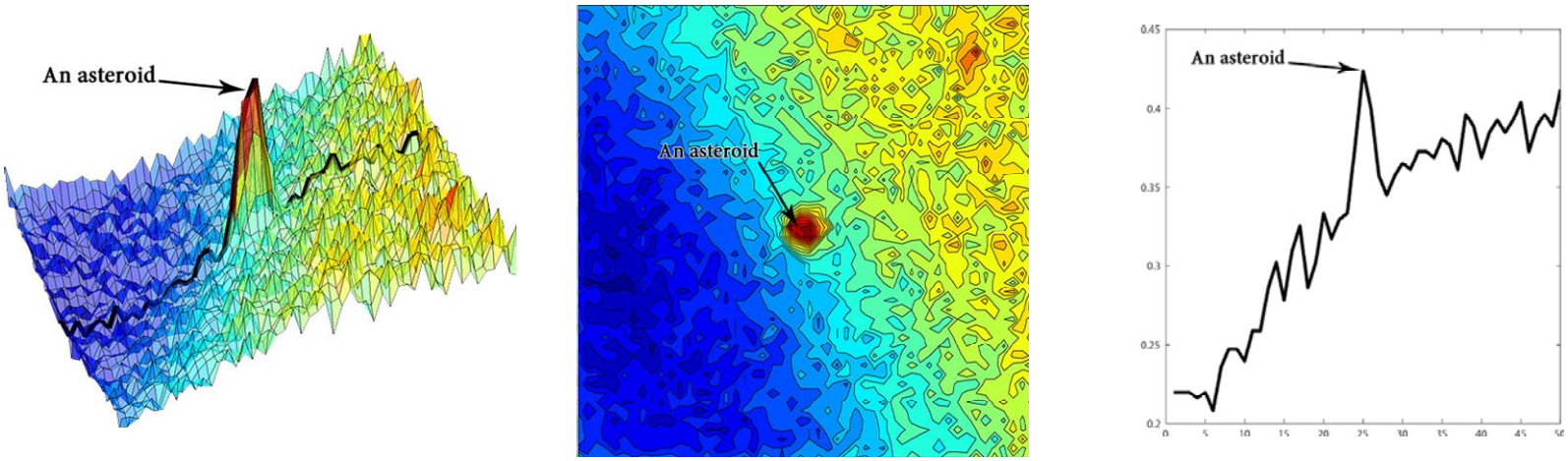

Fig. 3.3 Asteroid's signal on the noise flat substrate

Probability of photons getting in CCD-matrix pixel

$$\upsilon_{ikt}(\Theta) = \Delta^2_{CCD}(A_{noise}x_{ikt} + B_{noise}y_{ikt} + C_{noise}) + p_1 F_{xi}(x_t;\sigma^2)F_{yk}(y_t;\sigma^2_{ph}) = I_{ikts} + I_{iktnoise}, \qquad (3.9)$$

where $-\Delta_{CCD} = \Delta_x = \Delta_y$ the size of the region of ik-pixel of CCD-matrix according to x/y coordinates;

Noise flat substrate model

$$\upsilon^*_{iktnoise}(\theta) = A^{\text{int}}_{noise}x_{ikt} + B^{\text{int}}_{noise}y_{ikt} + C^{\text{int}}_{noise} \qquad (3.10)$$

where $\upsilon^*_{iktnoise}$ – empirical fall frequency of noise photons in ik-pixel of CCD-matrix; $A^{\text{int}}_{noise} = \Delta^2_{CCD}A_{noise}$; $B^{\text{int}}_{noise} = \Delta^2_{CCD}B_{noise}$; $C^{\text{int}}_{noise} = \Delta^2_{CCD}C_{noise}$ – integral parameters of плоской шумовой подложки determining parameters of noise distribution in the region of ik-pixel of CCD-matrix; x_{ikt}, y_{ikt} – mean coordinates of ik-pixel of CCD-matrix in the range of intraframe processing strobe; $\theta^T = (A^{\text{int}}_{noise}, B^{\text{int}}_{noise}, C^{\text{int}}_{noise})$ – column vector of integral parameters of the noise flat substrate параметров плоской шумовой подложки.

Estimation of asteroid's apparent brightness after its signal's amplitude

Estimation of asteroid's apparent brightness after its signal's amplitude. Introduction of a new double-band, piecewise-linear model representing dependence of visible asteroid brightness' value on its signal's amplitude on CCD-frame. The launch of the present model is stimulated by the fact, that the application of linear single-band model of photometric scaling for a wide range of amplitude values reduces precision of visible brightness evaluation for small amplitudes (appropriate to the asteroids' signal), while the application of quadratic single-band model of photometric scaling doesn't increase the precision rate as well. The best coefficients of the present double-band, piecewise-linear model are determined by LSM. The method is used in CoLiTec module of apparent brightness' estimation and permits to improve the precision of apparent brightness' estimation from asteroids in small amplitudes area (15-20%).

Estimation of asteroid's apparent brightness after its signal's amplitude

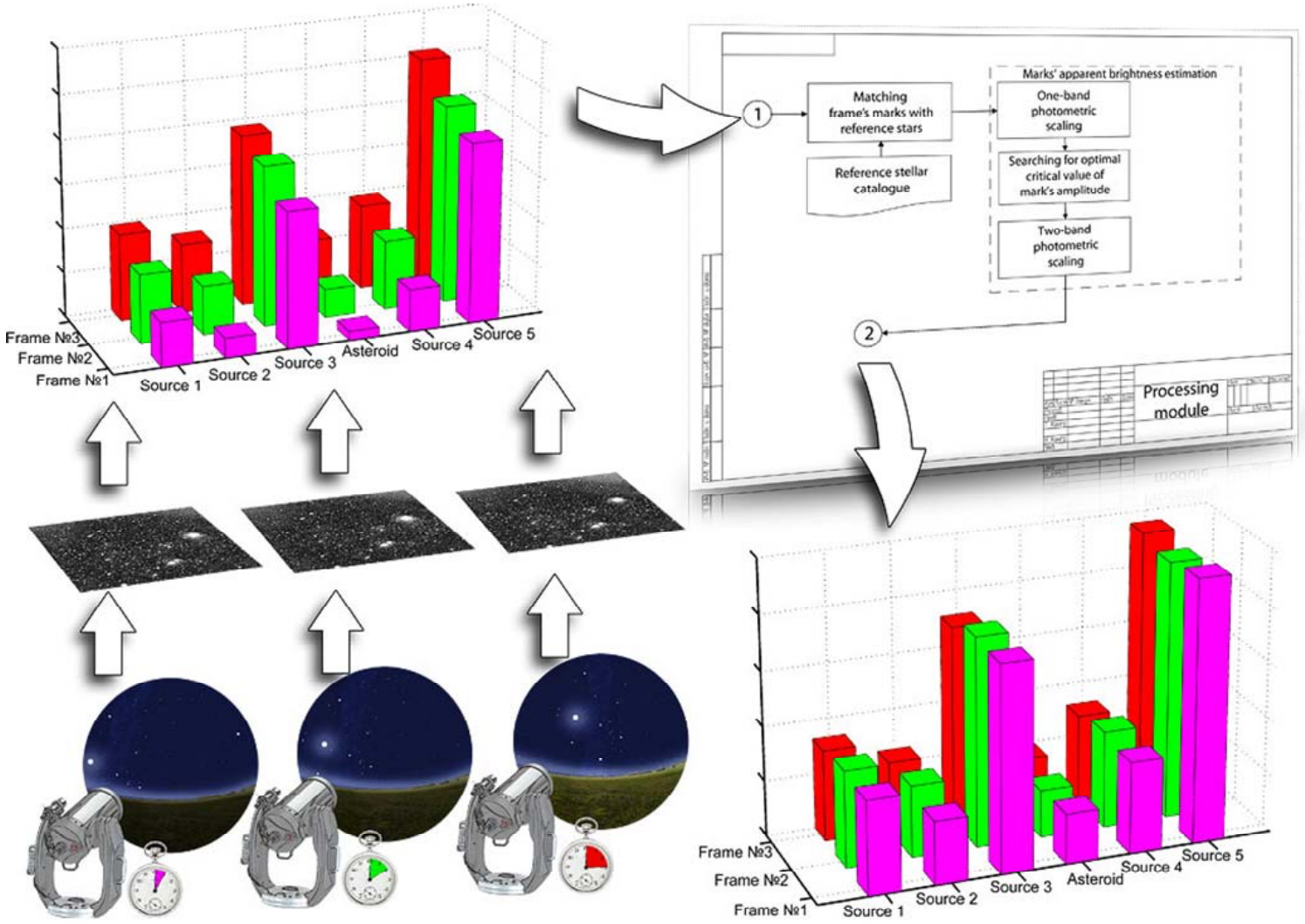

Fig 4.1

Estimation of asteroid's apparent brightness after its signal's amplitude (continuation)

Relation between estimation of signals' apparent brightness on one CCD-frame and their amplitudes

$$m_{1t} = m_{2t} - 2{,}5\ell g \frac{A_{1t}}{A_{2t}}, \tag{4.1}$$

where m_{1t}, m_{2t} – estimation of signals' apparent brightness (in magnitudes); A_{1t}, A_{2t} – marks' amplitudes matching given signals.

Single-band model of photometric scaling of signal's amplitude into apparent brightness' estimation

$$m_{eit} = m_{0t} + k_{phot1t} A_{\ell git}, \tag{4.2}$$

where $A_{\ell git} = -2{,}5\ell g A_{it}$ – measured of reference star's apparent brightness (A_{it} – mark's amplitude matching optical signal from the present star); m_{eit} – magnitude' s estimation of i-mark on the t-frame; m_{0t} – photometric zero-mark (star's apparent brightness with optical signal matching single amplitude mark under present observation's conditions); k_{phot1t} – scaling coefficient.

LSM-estimation of single-band photometric scaling coefficients

$$\Phi(m_{0t},\, k_{phot1t}) = \sum_{i=1}^{N_{stt}} (m_{0t} + A_{\ell git} k_{phot1t} - m'_{k(it)})^2 \xrightarrow[m_{0t},\, k_{phot1t}]{} \min. \tag{4.3}$$

$$\theta_{ephot} = (F_t^T F_t)^{-1} F_t^T \tilde{Y}_{phot}, \tag{4.4}$$

Estimation of asteroid's apparent brightness after its signal's amplitude (continuation)

$\tilde{Y}_{phot} = (m'_{1(1t)},...,m'_{k(it)},...,m'_{N_{stt}(N_{phot}t)})$ – group of catalog's estimation of apparent brightness of stars matching t-frame's marks; $m'_{k(it)}$ – apparent brightness' estimation of k - reference star from star catalog matching i -mark on t-frame; N_{stt} – quantity of reference stars matching the marks used to identify the coefficients of photometric scaling; N_{phott} – quantity of marks matching with reference stars and used to identify coefficients of photometric scaling ($N_{phott} = N_{stt}$).

Conditions of marks' selection for the next LSM step

$$\left|m'_{k(it)} - m_{eit}\right| \le k_{ph}\sqrt{(\sum_{i=1}^{N_{stt}}(m'_{k(it)} - m_{eit})^2/(N_{stt}-1))}, \qquad (4.5)$$

where k_{ph} – threshold coefficient of rejection; $\sqrt{(\sum_{i=1}^{N_{stt}}(m'_{k(it)} - m_{eit})^2/(N_{stt}-1))}$ – estimation of mean square deviation of mark's apparent brightness' estimation; $m_{eit} = m_{0t} + k_{phot1t}A_{\ell git}$ – smoothed apparent brightness' estimation of i -mark matching k -star on t -frame.

Double-band, piecewise-linear model of photometric scaling

$$\begin{cases} m_{eit} = m_{01t} + k_{phot1t}A_{\ell git}, & A_{it} \ge A_{crt}; \\ m_{eit} = m'_{1t} + k_{phot2t}(A_{\ell git} - \overline{A}_{\ell g1t}), & A_{it} < A_{crt}, \end{cases} \qquad (4.6)$$

where $\overline{A}_{\ell g1t} = -2{,}5\ell g A_{crt}$ (7), A_{crt} – critical value of signal's amplitude.

Partial derivatives matrix for model's second range

$$F_{2t}^T = \left\| (A_{\ell g1t} - \overline{A}_{\ell g1t}) \dots (A_{\ell git} - \overline{A}_{\ell g1t}) \dots (A_{\ell gN_{st}2t} - \overline{A}_{\ell g1t}) \right\|, \qquad (4.7)$$

where N_{st2t} – quantity of stars matching marks with amplitudes smaller than value.

Comparison of single-band and double-band models of photometric scaling

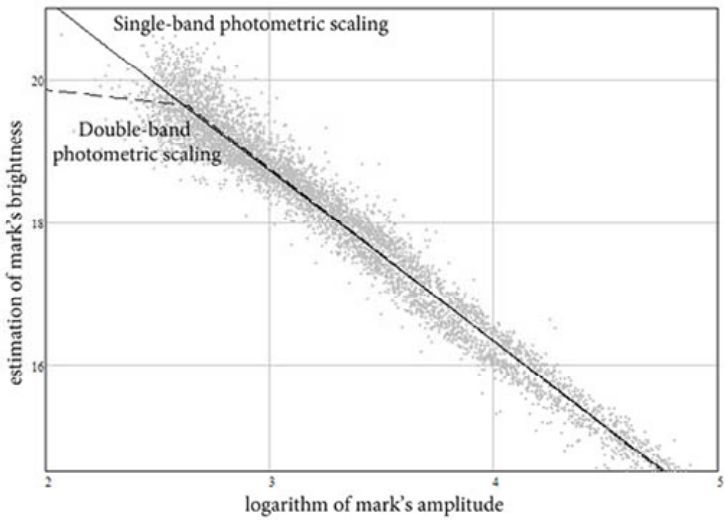

Fig. 4.2 Dependence of apparent brightness' estimation upon amplitude

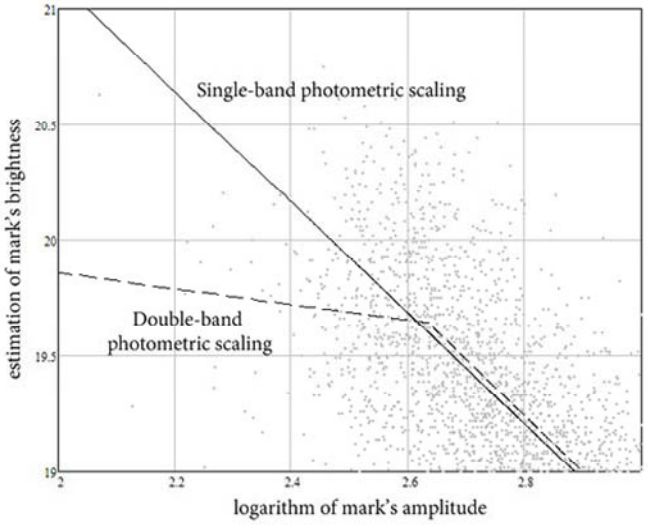

Fig. 4.3 Dependence of apparent brightness' estimation upon amplitude. Small amplitudes' area

A double-step method of asteroid's detection

A double-step method of asteroid's detection**.** Method is based on the statistics accumulation basis proportional to the signal energy along the possible paths of the object motion. The present signal accumulation is provided due to implementation of multiple-valued transformation of object coordinates allowing multistage implementation. Multiple-valued transformation also allows accumulating signals along all the possible motion paths of celestial bodies. A multistep computational scheme stabilizes computational cost level. According to the set motion model, physically observed spatial domain divides into crossing space-time domains (spatial domains moving from one frame to another). The division doesn't permit asteroid to escape from any of those domains during detection stage. Each domain has its own storage. The signals from celestial objects are stored in all the storages of corresponding domains.

At the first step, separate tracks gather in classes. All tracks of the same straight line are gathered in one class. The studying space-time domains will be chosen according to the straight line with detected celestial objects on it.

This method differs from the prototype in the following:

a) Rejection of signals from objects, motionless on T-frames before detection process, through creation of an inner catalog for motionless objects. This process cuts down computational cost of detection by reducing the quantity of processed marks; reduces the quantity of false asteroid's detections.

b) Signal marks getting into two or three (not into one, as it was before) strobes according to the traverse distance and their reference attitude (because of the record of eventual errors in objects' coordinates estimation).

c) The estimation of apparent brightness of objects's signal is used as accumulative statistic. The value of this estimation for the same asteroid doesn't depend (weakly depends) on changes in observation conditions from one frame to another within one series of observation.

The present method permits to improve the quality of moving objects' detection matching the quality of motionless objects' detection.

CoLiTec software method uses module of motionless objects' catalog creation and module of preliminary tracks' detection.

Method of asteroid's detection

Method of asteroid's detection is based on the statistics accumulation basis proportional to the signal energy along the possible paths of the object's motion

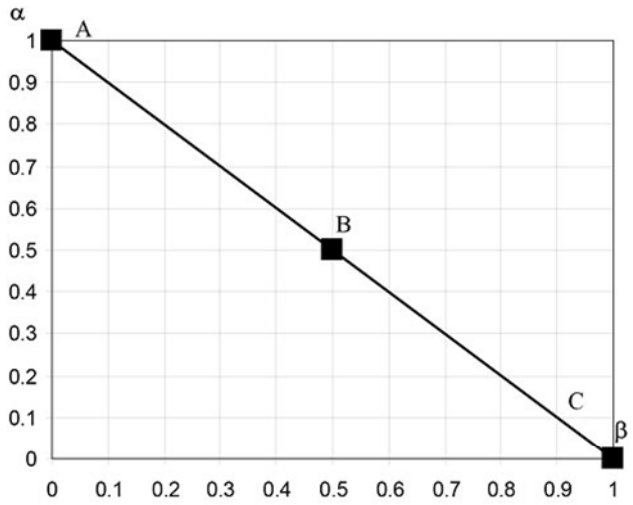

Fig. 5.1 Track's display

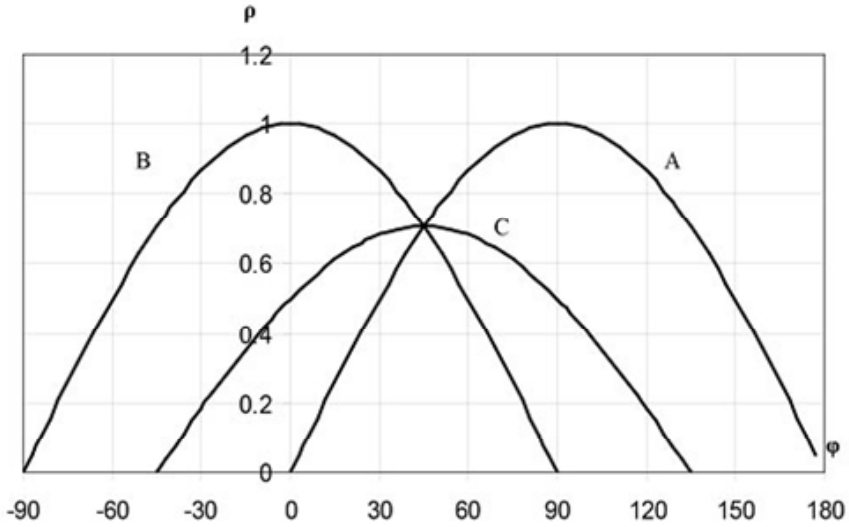

Fig. 5.2 Display of image's points in the plane of traverse angles and distance

Amplitude-Coordinates Method

Introduction of Amplitude-Coordinates Method of detection and estimation of asteroid's tracks parameters after the group of one strobe's marks from the second step of preliminary asteroids' detection, with accumulated amplitude exceeding the threshold.

Detection of an asteroid starts after the estimation of its track's parameters. The method of asteroids' detection on each frame chooses "the best" mark for extension of the path. "The best" mark should have little deviation (kinematic constituent) from asteroid path, while the amplitude value of "the best" mark (valuation of the apparent brightness of the object relevant to the mark) should not be very different from the amplitude of the other marks which belong to the given path (amplitude constituent). Application of this amplitude constituent is connected with big amplitude variation of signals from asteroids by rapid change of observation conditions within the time of observation.

Method is used in the module of amplitude and coordinate detection (ACD) of CoLiTec software and permits to reduce (in several times) quantity of false tracks sent to the CoLiTec visual control of results module.

Static objects detection

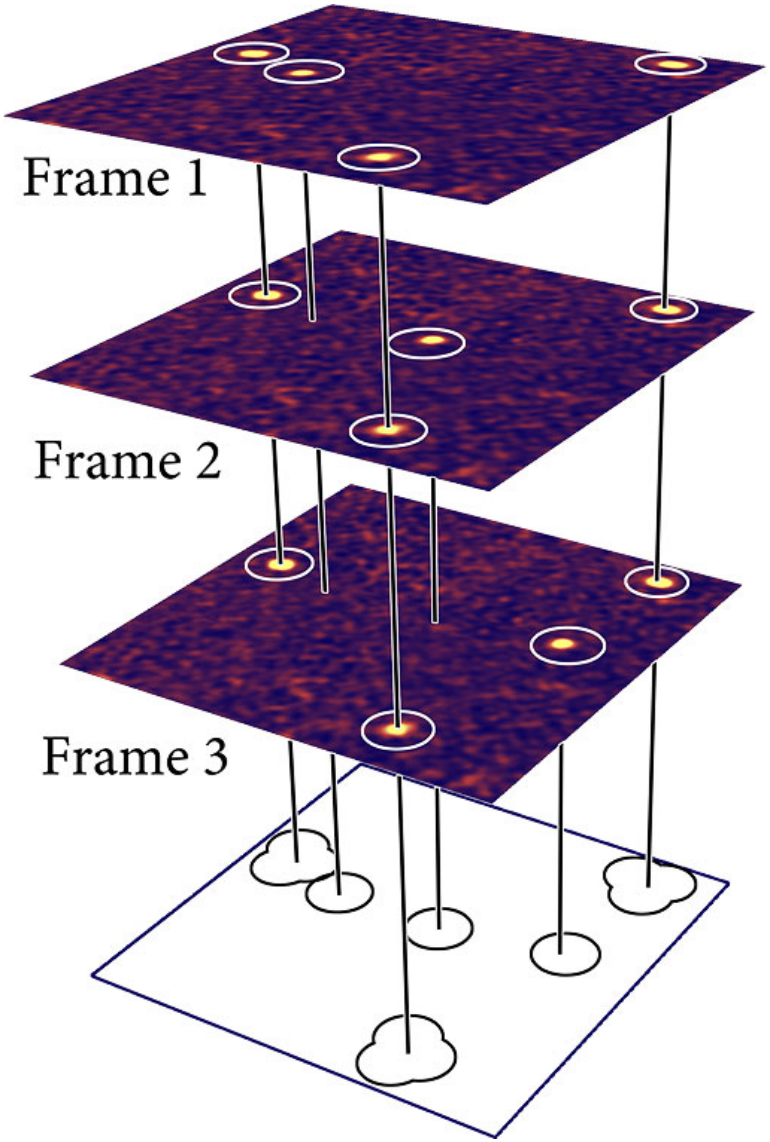

Algorithm for moving object detection

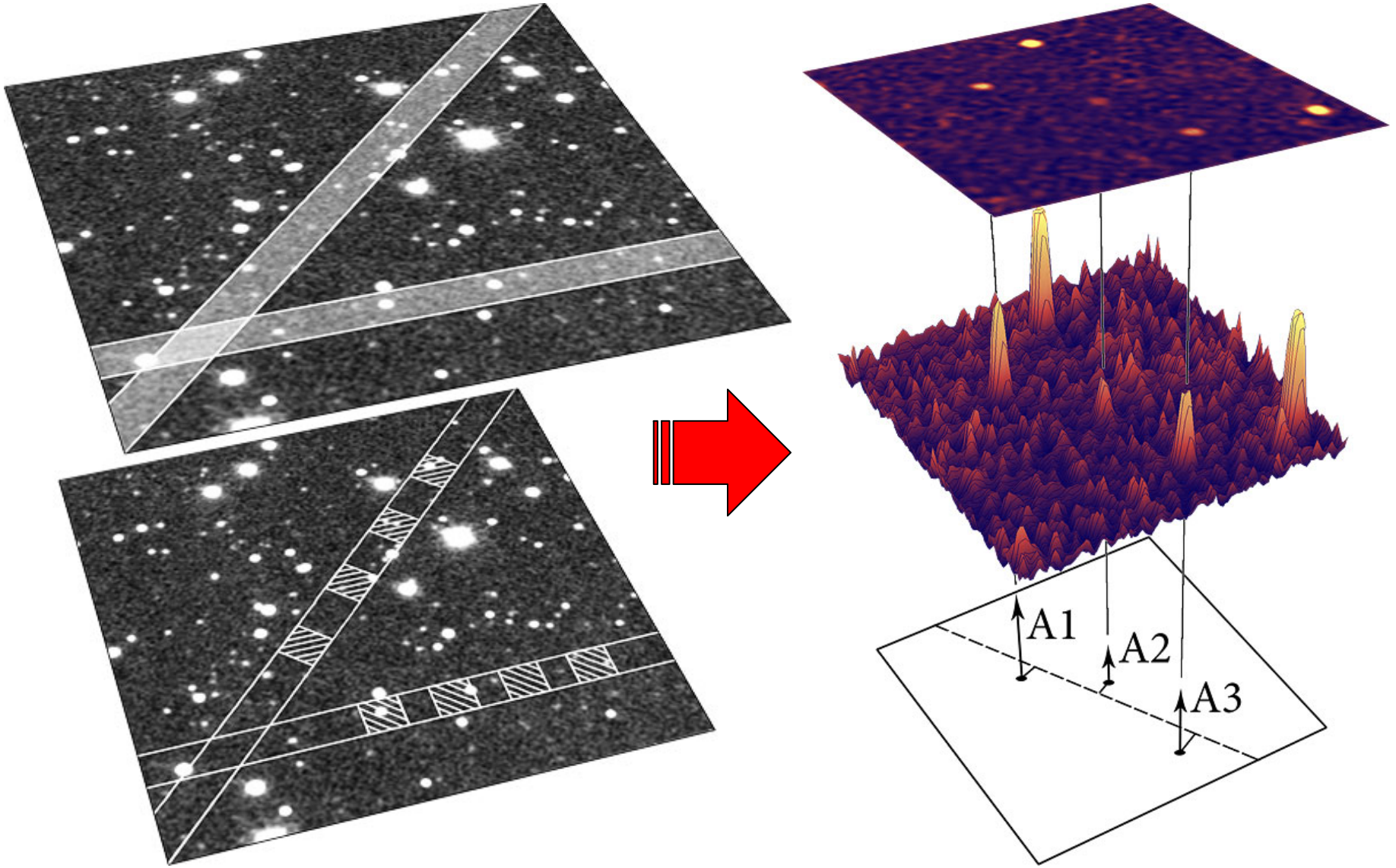

Decision rules of asteroid's detection on the series of frames

Decision rule of asteroid's detection on the series of frames with nonzero probability of asteroid's mark skipping on separate frames

$$\sum_{t=1}^{K}\gamma_{tjx}(x_{kt(j)}-x_{ejt})^2+\sum_{t=1}^{K}\gamma_{jy}(y_{kt(j)}-y_{ejt})^2+\sum_{t=1}^{K}\gamma_{ja}(A_{kt(j)}-A_{\theta ejmean})^2\geq Tr'_{tre}(K), \qquad (6.1)$$

where $Tr'_{tre}(K)=Tr_{tre}-\sum_{t=K+1}^{T}\ell n\frac{1-D_{\theta t(j)}}{1-F_t}$ – asteroid's detection threshold with asteroid's marks formation on K from T frames.

Decision rule of asteroid's detection on the series of frames with asteroid's marks present on all the frames

$$\sum_{t=1}^{T}\gamma_{tjx}(x_{kt(j)}-x_{ejt})^2+\sum_{t=1}^{T}\gamma_{jy}(y_{kt(j)}-y_{ejt})^2+\sum_{t=1}^{T}\gamma_{ja}(A_{kt(j)}-A_{\theta ejmean})^2\geq Tr_{tre}, \qquad (6.2)$$

where Tr_{tre} – asteroid's (track's) detection threshold, experimentally determined after Neiman-Pirson criteria;

$$\gamma_{tjx}=1/\sigma^2_{tjx};\ \gamma_{tjy}=1/\sigma^2_{tjy}; \qquad (6.3)$$

–weighting factors directly proportional to the accuracy of objects' coordinates estimation that depends on their location on the frame and SNR of this object's;

$$\gamma_{tja}=1/\sigma^2_{tja} \qquad (6.4)$$

– weighting factors depending on the accuracy of signals' amplitude estimation.

OLDAS - OnLine Data Analysis System

1. Management of FITS files
2. Processing images in the real time
3. Obtaining results in 30 minutes after end of astronomical twilight
4. Working with online catalogues via VizieR
    1. Identification known static object on image (USNO B1.0, SDSS v8)
    2. Supernova search – labeling unknown static objects near galaxies
    3. Photometry all known variable stars, patrol of cataclysmic VS
5. Sending measurements to MPC
6. Inspection detected objects via web-interface*

** - plans for the near future*

CoLiTec *lite* version

CoLiTec *lite* may be available to GAIA-FUN participants in late of 2012

1. Working with really large field of views, up to 10 degrees^2
2. All mathematics from original CoLiTec which used by our surveys (A50, D00, H15)
3. Precise astrometry on edges of images with huge distortion
4. Track and stack technique for measuring FMO
5. Search for moving objects on series of images
6. Identification all moving objects via MPC online service
7. Showing NEO rating for all unknown objects
8. Upload online catalogs via VizieR*

Minor Planet Center statictics

	Observatory	Number of observations	Numbered asteroids	Unnumbered asteroids
1	Mt. Lemmon Survey (G96)	1 761 673	175 435	64 545
2	Lincoln Laboratory ETS (704)	1 715 560	119 388	5 412
3	Catalina Sky Survey (703)	1 350 625	123 074	13 638
4	Pan-STARRS 1 (F51)	1 274 273	162 396	52 931
5	Steward Observatory (691)	688 692	87 154	26 097
6	Siding Spring Survey (E12)	214 220	29 161	1 968
7	Purple Mountain Observatory (D29)	185 968	37 719	2 839
8	**ISON-NM Observatory (H15)**	**135 482**	**27 313**	**3 549**
9	Črni Vrh Observatory (106)	85 181	18 008	774
10	LPL/Spacewatch II (291)	52 058	8 694	4 302

Overall statistics for 2011 year

Minor Planet Center statictic

	Observatory	Number of observations	Numbered asteroids	Unnumbered asteroids
1	Pan-STARRS 1 (F51)	1 191 224	159 197	33 127
2	Mt. Lemmon Survey (G96)	997 574	110 918	26 373
3	Catalina Sky Survye (703)	893 295	86 394	5 814
4	Lincoln Laboratory ETS (704)	791 955	61 353	1 027
5	Steward Observatory (691)	458 421	58 461	11 912
6	Siding Spring Survey (E12)	204 520	31 524	1 451
7	**ISON-NM Observatory (H15)**	**57 580**	**12 940**	**839**
8	Črni Vrh Observatory (106)	42 493	9 475	312
9	Oukaïmeden Observatory (J43)	37 019	7 778	534
10	Les Engarouines Observatory (A14)	22 648	5 853	397

Statistics for January - July 2012

Statistics of residuals

	Observatory	R.A. (arcsec)	Decl. (arcsec)
1	Pan-STARRS 1 (F51)	+0.08 +/- 0.16	+0.06 +/- 0.17
2	Mt. Lemmon Survey (G96)	-0.01 +/- 0.33	+0.04 +/- 0.29
3	Catalina Sky Survey (703)	-0.22 +/- 0.66	+0.02 +/- 0.62
4	Lincoln Laboratory ETS (704)	+0.40 +/- 0.66	+0.43 +/- 0.64
5	Steward Observatory (691)	-0.12 +/- 0.32	+0.10 +/- 0.30
6	Siding Spring Survey (E12)	-0.02 +/- 0.50	+0.30 +/- 0.49
7	**ISON-NM Observatory (H15)**	**-0.07 +/- 0.50**	**+0.03 +/- 0.53**
8	Črni Vrh Observatory (106)	+0.01 +/- 0.37	-0.10 +/- 0.34
9	Oukaïmeden Observatory (J43)	+0.28 +/- 0.62	+0.19 +/- 0.49
10	Les Engarouines Observatory (A14)	+0.05 +/- 0.38	-0.02 +/- 0.32

Statistics for January – September 2012

Results of our survey program

- Obtained more than 265 000 observations
- Discovered more than 1000 MBA (provisional designation)
- Two near-Earth asteroids 2010 RN80 and 2011 QY37 (both Amors)
- Long-period comet C/2010 X1 (Elenin)
- Short-period near-Earth (q=1.24) comet P/2011 NO1 (Elenin)
- Dozen Jovian trojans


Dust cloud - the debris of the comet C/2010 X1
©Rolando Ligustri

NEAs photometry

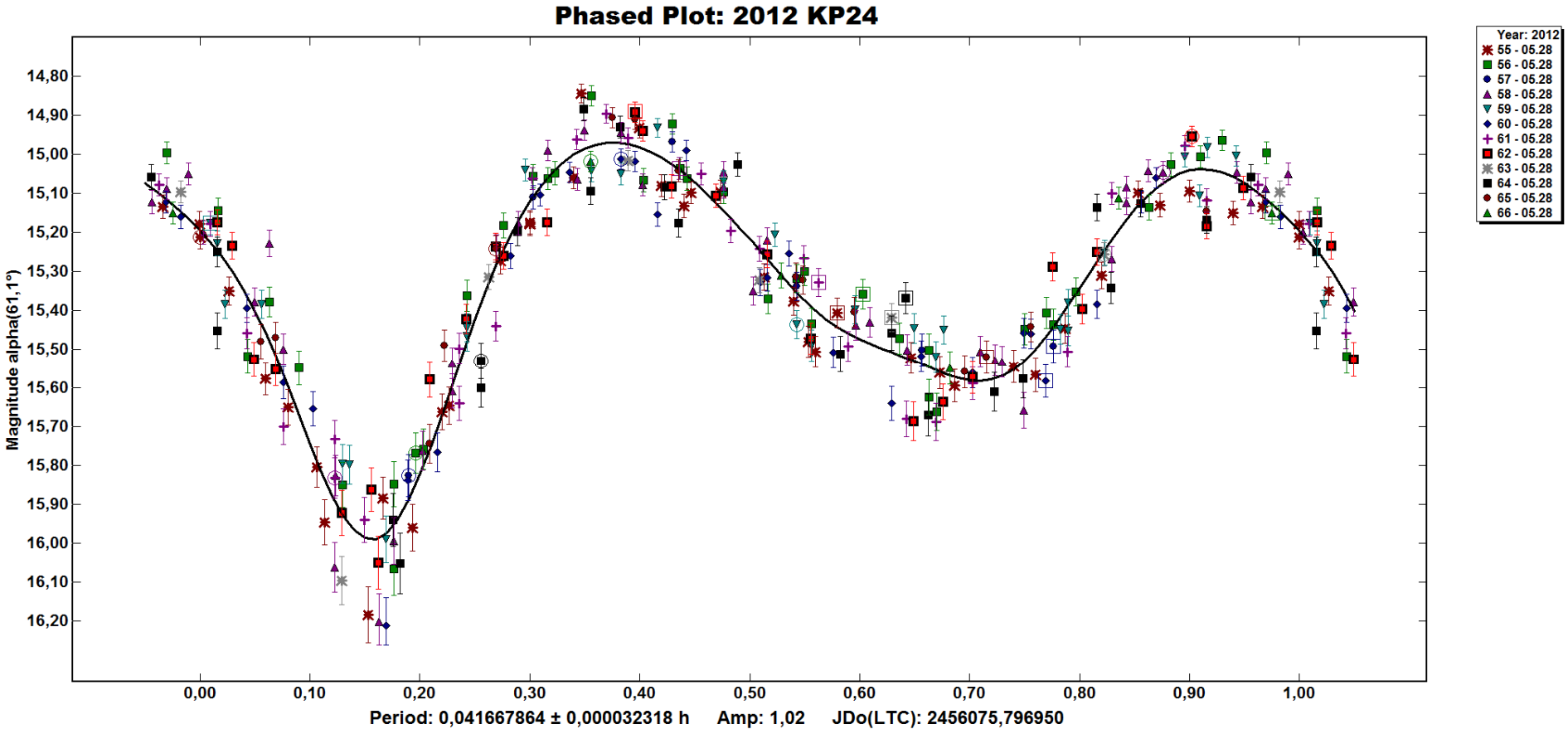

Rotation period — 150 sec

NextGen survey telescope

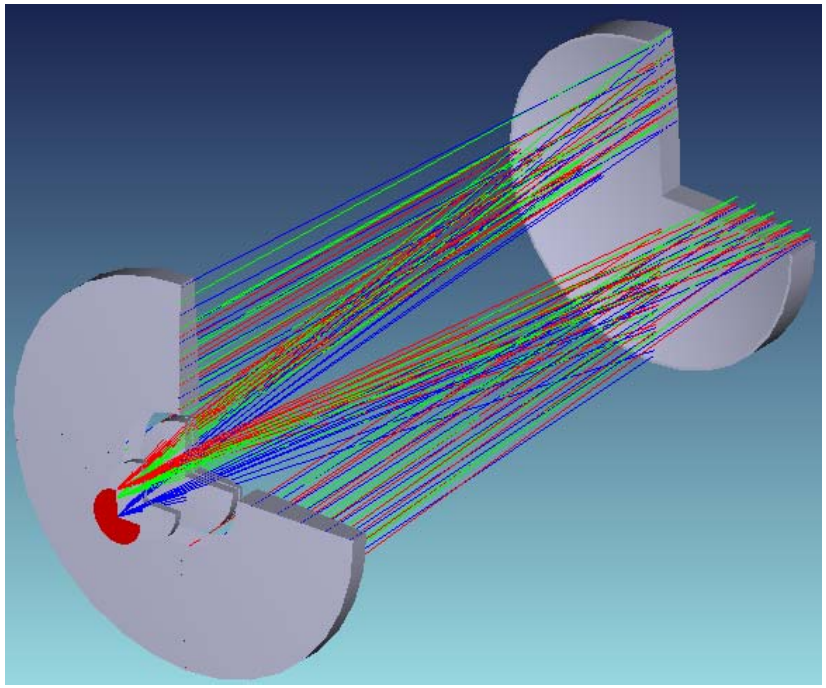

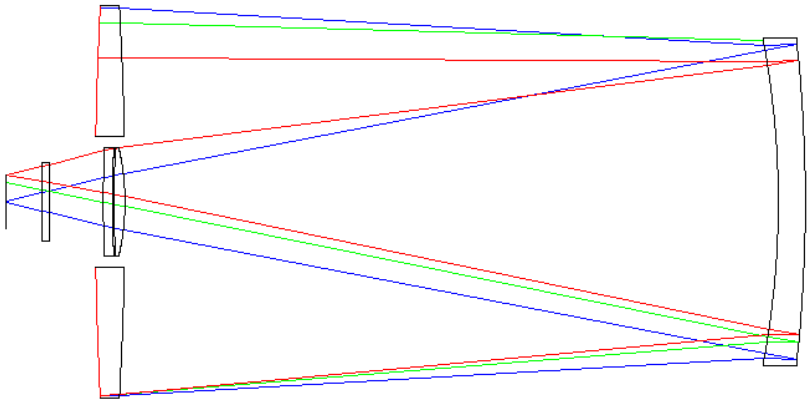

Aperture, mm	600
Focal ratio	f/2.0
Angular field diameter, degrees	4
Linear field diameter, mm	52.4
Spectral range, nm	450-850
Back focal length, mm	159
Central obscuration ratio	0.33
Relative illum. on the edge of FOV	0.83
Distortion, %	0.14
Optical system's length, mm	1344

Plans for the future

• Improving CoLiTec pipeline — ability to detection more faint and fast moving objects, decreasing processing time and using multi-processor clusters (OpenCL)

• **Adding automatic pipeline for follow-up (observations & measurements) important Solar System objects (critical list, NEOCP, Gaia)**

• Replacing our C-18 by our new survey telescope SANTEL 0.65-m f/2.0: more «deeper» survey with larger sky coverage

• Extracting more by-products from the survey's images

Work in progress...

ISON follow-up network

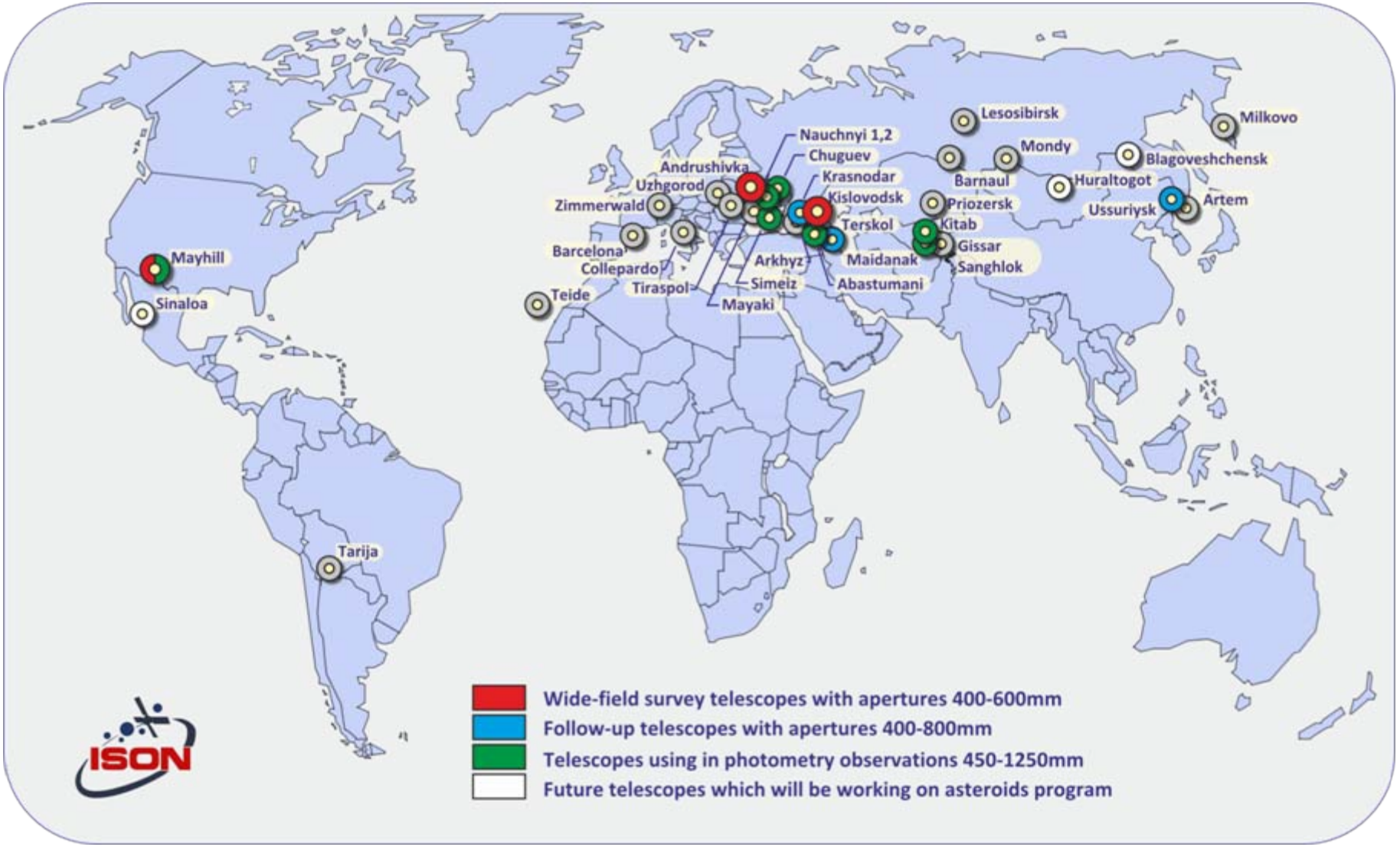

Follow-up telescopes

Andrushivka Astronomical Observatory (A50)

Aperture – 600 mm
Focus lenght – 2400 mm
Focal ratio – f/4
CCD – FLI PL4301
FOV – 72'x72'
Image scale – 2.07"/pix

ISON-Ussuriysk Observatory (C15)

Aperture – 500 mm
Focus lenght – 1150 mm
Focal ratio – f/2.3
CCD – FLI PL9000
FOV – 110'x110'
Image scale – 2.15"/pix

Follow-up telescopes

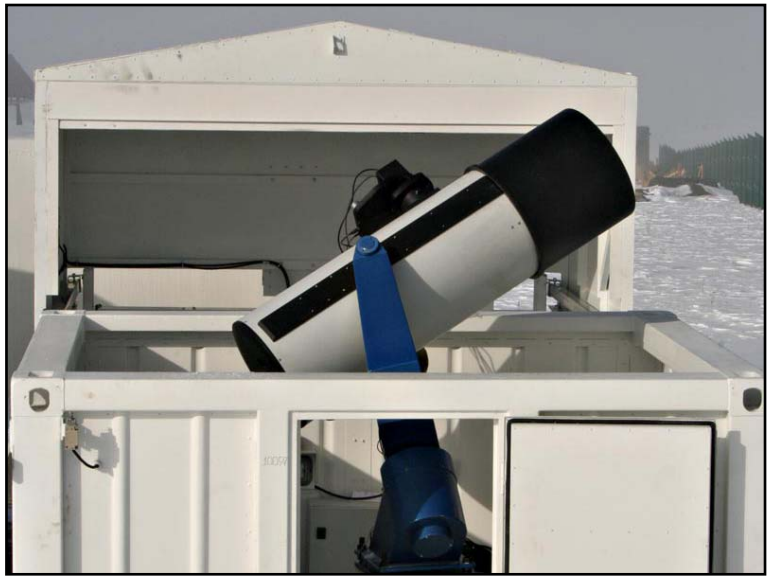

ISON-Kislovodsk Observatory (D00)

Aperture – 40 mm
Focus lenght – 1200 mm
Focal ratio – f/3
CCD – FLI ML9000-65
FOV – 106'x106'
Image scale – 2.06"/pix

ISON-Terskol Observatory (D05)

Aperture – 800 mm
Focus lenght – 2224 mm
Focal ratio – f/2.78
CCD – FLI ML1001E
FOV – 38'x38'
Image scale – 2.23"/pix

Thank you!

Leonid Elenin
l.elenin@gmail.com
www.spaceobs.org/en

Vadim Savanevych
vadym@savanevych.com
www.neoastrosoft.com

Igor Molotov
im62@mail.ru
www.astronomer.ru